Communication

Silicon Nanowire Array Photoelectrochemical Cells

Adrian P. Goodey, Sarah M. Eichfeld, Kok-Keong Lew, Joan M. Redwing, and Thomas E. Mallouk

J. Am. Chem. Soc., **2007**, 129 (41), 12344-12345• DOI: 10.1021/ja073125d • Publication Date (Web): 25 September 2007

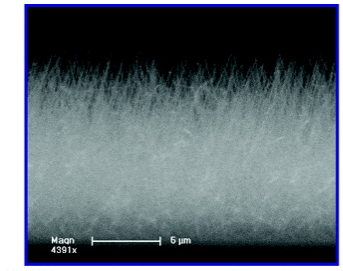

Silicon Nanowire Array

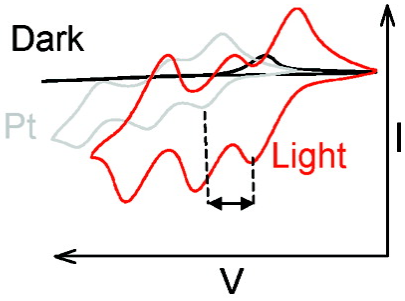

J|A|C|S
COMMUNICATIONS

Published on Web 09/25/2007

Silicon Nanowire Array Photoelectrochemical Cells

Adrian P. Goodey,[†] Sarah M. Eichfeld,[‡] Kok-Keong Lew,[‡] Joan M. Redwing,*[,‡] and Thomas E. Mallouk*[,†]

Departments of Chemistry and Materials Science and Engineering, The Pennsylvania State University, University Park, Pennsylvania 16802

Received May 3, 2007; E-mail: tom@chem.psu.edu; jmr31@psu.edu

The development of efficient but inexpensive solar cells is an important current challenge. Semiconductor nanowires provide new opportunities for addressing the cost and efficiency issues of conventional photovoltaic (PV) and photoelectrochemical (PEC) cells. Recent studies of semiconductor nanowire growth[1−3] show that it is relatively easy to make arrays of vertically oriented single crystals, which should be less susceptible to the grain-boundary recombination problem of polycrystalline solar cells. Moreover, relaxed lattice matching requirements in nanowires allow one to make epitaxial nanowire heterostructures,[4−6] thereby enabling better solar spectral utilization with multi-band gap nanowires.

The "bed of nails" geometry of a vertical nanowire array also offers significant advantages over a planar semiconductor photoelectrode. One important consequence is the potential for all photogenerated carriers to be created within the space charge region of the semiconductor, regardless of the light penetration depth. The doping density and depletion layer width can thus be tailored independently of the absorption length.[7] This geometry is also well suited to excitonic cells, in which vertical nanowires minimize exciton diffusion distances while providing an uninterrupted conduction pathway.[8,9] For these reasons, semiconductor nanoarchitectures have been increasingly studied for their potential solar energy applications. Indeed, nanocrystal hybrid PVs[9] and nanowire dye-sensitized solar cells[10−13] have already been reported. To date, however, the only reported solar energy application of silicon nanowire (SiNW) arrays relies on a non-transferable wafer etching technique.[14]

We previously reported the growth of SiNW arrays using anodic aluminum oxide (AAO) membranes as templates,[3] and demonstrated p- and n-type doping.[15,16] In our first attempts to make liquid junction PECs by this technique, we electrodeposited 50 μm long Co nanowires in the membranes and capped them with 250 nm Au segments (Figure 1). Si nanowires were then grown from SiH_4 at 500 °C by the vapor−liquid−solid (VLS) method.[17] The back metallic contact was insulated with a combination of glass tubing and epoxy, leaving only the nanowire-bearing face of the SiNW electrode exposed. After etching away the exposed Au catalyst from the tips of the nanowires using aqueous tri-iodide, the electrochemical response shown in Figure 1C was obtained. The SiNW photoelectrode was immersed in a glass vial containing a solution of 2 mM tris(2,2′-bipyridyl)ruthenium(II) hexafluorophosphate ($Ru(bpy)_3^{2+}$) (bpy = 2,2′-bipyridyl) and 100 mM tetra(*n*-butyl)ammonium tetrafluoroborate ($TBABF_4$) in dry CH_3CN. A $Ag/AgNO_3$ (in CH_3CN) reference and a Pt gauze counter electrode completed the three-electrode cell. Ar was bubbled through the cell to deoxygenate the solution prior to electrochemical measurements, and a positive pressure of Ar was maintained at all times. A Hg/Xe arc lamp was used as the light source, yielding an

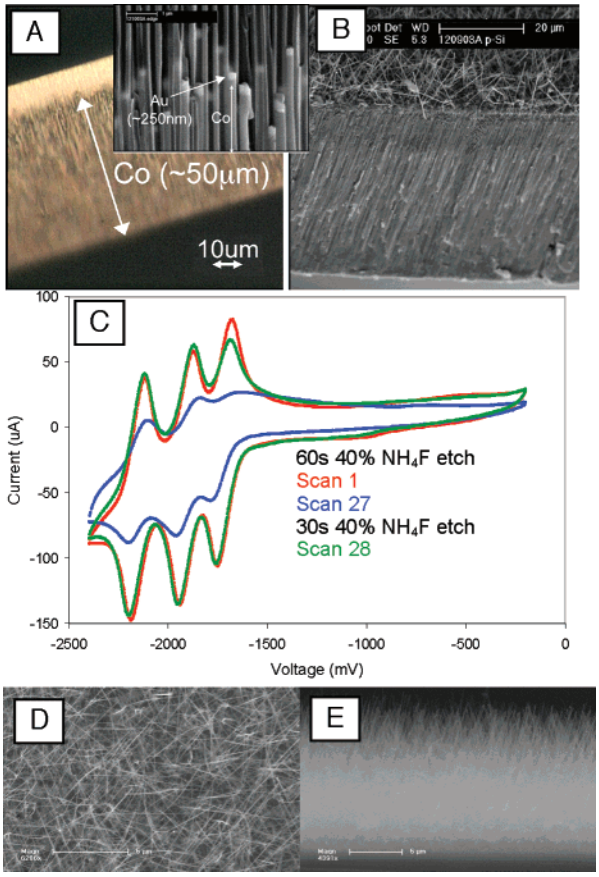

Figure 1. (A) Cross sectional view of AAO membrane showing the typical uniformity of electrodeposited Co. Inset SEM shows individual Co wires and their Au caps. (B) SEM showing a cross section of the membrane in panel A after VLS growth of p-Si nanowires, which protrude 10−15 μm beyond the top of the membrane. (C) Cyclic voltammetry of an illuminated p-Si/AAO nanowire array electrode in $Ru(bpy)_3^{2+}$ solution, showing the effect of fluoride etching. Top (D) and side (E) view scanning electron micrographs of a free-standing p-Si nanowire array grown on Si.

illumination of 0.84 W/cm^2 at the cell surface. Surface oxide was etched from the SiNW array using aqueous ammonium fluoride.

In the case of the SiNW array grown in AAO, light and dark currents were identical (Figure 1C). Repeated voltammetric cycling covered the Si surfaces of the electrode with an insulating oxide, resulting in lower dark current. The recovery of this current with Etching indicates that neither exposed Au nor Co is the source of the dark current. Rather, it is likely that the SiNWs are degeneratively doped by Al from the AAO membrane, and therefore current rectification does not occur at the SiNW/solution interface.[18]

To grow SiNW arrays with lower doping density, a p-type (111) Si wafer with a 1 nm Au film was used as the substrate. Doping

[†] Department of Chemistry.
[‡] Department of Materials Science & Engineering.

10.1021/ja073125d CCC: $37.00

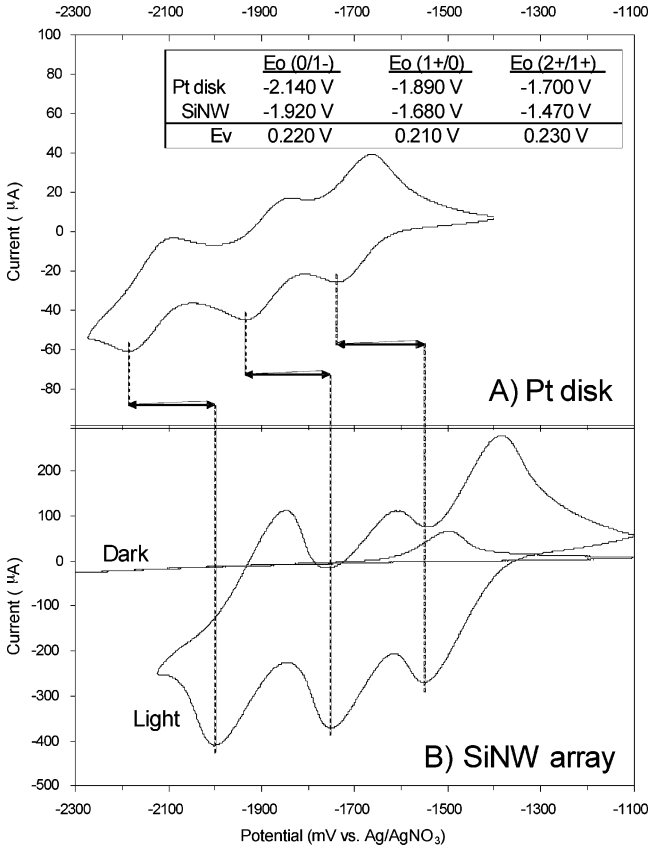

Figure 2. Cyclic voltammograms (200 mV/s) of (A) a Pt disk electrode and (B) a silicon nanowire array photocathode, both light and dark, as indicated. (Inset) Midpoint potentials (E_0) of the $Ru(bpy)_3$ anodic and cathodic peaks at the metallic and semiconductor electrodes and the calculated photovoltages (E_v).

was controlled by simultaneous introduction of trimethylboron (TMB) at a TMB/SiH_4 volume ratio of 2×10^{-4}. Micrographs of the resulting nanowires are shown in Figure 1D, E. The nanowires are approximately 14 μm long, with an average diameter of 57 $\pm$ 12 nm. Ohmic contact was made to the back side of the substrate via an evaporated Au film, which was then connected to a copper wire using conductive Ag epoxy.

Figure 2 shows cyclic voltammograms obtained from this p-SiNW array. Panel A shows the three cathodic and anodic peaks of the $Ru(bpy)_3^{2+}$ redox couple at a Pt disk electrode. Panel B shows analogous $i-V$ curves from the SiNW array photocathode, both illuminated and in the dark. Reduction of $Ru(bpy)_3^{2+}$ by the illuminated SiNW array occurs at potentials significantly more positive than at the Pt electrode. In the dark, the SiNW array exhibits negligible cathodic current in the same potential range. Both these observations are consistent with the behavior of a p-type Si photocathode. The inset table lists the formal potentials (E_0) of $Ru(bpy)_3^{2+}$ measured at the Pt disk and at the illuminated SiNW array, and the calculated photovoltages (E_v). E_0 values were measured as the mean of the peak potentials at each electrode; E_v values were calculated as the difference between corresponding E_0 values. On average, photoassisted reductions at the SiNW array occur 220 mV positive of the same reductions at the Pt disk electrode. At scan rates between 20 and 2000 mV/s, the photocurrent density at the SiNW array is approximately twice that of a planar p-Si electrode (see Supporting Information). This is consistent with photocurrent generation from the top $\sim$ 5 μm of the high surface area SiNW array.

In the mass transport limited regime of the SiNW PEC, the measured E_v values correspond to the open circuit voltage (V_{oc}) of the cell. Although the observation of a significant photovoltage is encouraging, a V_{oc} of ca. 500 mV is observed for p-Si single-crystal electrodes under similar conditions.[19,20] Several explanations for the lower photovoltage of the nanowire photocathode are possible. One is that excessive doping results in an insufficiently thick space charge region, creating a leaky diode junction.[21] This hypothesis is supported by data from nanowires made with higher TMB/SiH_4 ratios. At a ratio of 7×10^{-4}, the photovoltage was 130 mV, and at 2×10^{-2}, no photovoltage (i.e., identical light and dark current) was observed. It is also possible that the introduction of boron from TMB increases the density of surface states at the nanowire surface, resulting in increased dark current. It may be possible to minimize such surface effects by increasing the nanowire diameter, thus decreasing the surface to volume ratio. Accordingly, current efforts are focused on optimizing the doping levels and nanowire dimensions. The effects of surface states must also be considered.

To our knowledge, this is the first observation of photoelectrochemical energy conversion at a SiNW array grown by VLS or related techniques. As such, it represents a step toward the ultimate goal of making inexpensive SiNW PEC cells and multijunction solid-state devices.

Acknowledgment. This work was supported by the Department of Energy under contract DE-FG02-05ER15749. A.P.G. thanks the Donors of the ACS Petroleum Research Fund for support of this research in the form of a postdoctoral fellowship.

Supporting Information Available: Scan rate dependence of the photocurrent and additional synthetic and experimental details. This material is available free of charge via the Internet at http://pubs.acs.org.

References

(1) Wu, Y.; Yan, H.; Huang, M.; Messer, B.; Song, J. H.; Yang, P. *Chem.—Eur. J.* **2002**, *8*, 1260−1268.
(2) Fuhrmann, B.; Leipner, H. S.; Hoeche, H.-R.; Schubert, L.; Werner, P.; Goesele, U. *Nano Lett.* **2005**, *5*, 2524−2527.
(3) Lew, K.-K.; Reuther, C.; Carim, A. H.; Redwing, J. M.; Martin, B. R. *J. Vac. Sci. Tech., B* **2002**, *20*, 389−392.
(4) Wu, Y.; Fan, R.; Yang, P. *Nano Lett.* **2002**, *2*, 83−86.
(5) Bjoerk, M. T.; Ohlsson, B. J.; Sass, T.; Persson, A. I.; Thelander, C.; Magnusson, M. H.; Deppert, K.; Wallenberg, L. R.; Samuelson, L. *Nano Lett.* **2002**, *2*, 87−89.
(6) Gudiksen, M. S.; Lauhon, L. J.; Wang, J.; Smith, D. C.; Lieber, C. M. *Nature* **2002**, *415*, 617−620.
(7) Kayes, B. M.; Atwater, H. A.; Lewis, N. S. *J. Appl. Phys.* **2005**, *97*, 114302/1−114302/11.
(8) Kannan, B.; Castelino, K.; Majumdar, A. *Nano Lett.* **2003**, *3*, 1729−1733.
(9) Huynh, W. U.; Dittmer, J. J.; Alivisatos, A. P. *Science* **2002**, *295*, 2425−2427.
(10) Baxter, J. B.; Aydil, E. S. *Appl. Phys. Lett.* **2005**, *86*, 053114/1−053114/3.
(11) Law, M.; Greene, L. E.; Johnson, J. C.; Saykally, R.; Yang, P. *Nature Mater.* **2005**, *4*, 455−459.
(12) Ravirajan, P.; Peiro, A. M.; Nazeeruddin, M. K.; Graetzel, M.; Bradley, D. D. C.; Durrant, J. R.; Nelson, J. *J. Phys. Chem. B* **2006**, *110*, 7635−7639.
(13) Law, M.; Greene, L. E.; Radenovic, A.; Kuykendall, T.; Liphardt, J.; Yang, P. *J. Phys. Chem. B* **2006**, *110*, 22652−22663.
(14) Peng, K.; Xu, Y.; Wu, Y.; Yan, Y.; Lee, S.-T.; Zhu, J. *Small* **2005**, *1*, 1062−1067.
(15) Lew, K.-K.; Pan, L.; Bogart, T. E.; Dilts, S. M.; Dickey, E. C.; Redwing, J. M.; Wang, Y.; Cabassi, M.; Mayer, T. S.; Novak, S. W. *Appl. Phys. Lett.* **2004**, *85*, 3101−3103.
(16) Wang, Y.; Lew, K.-K.; Ho, T.-T.; Pan, L.; Novak, S. W.; Dickey, E. C.; Redwing, J. M.; Mayer, T. S. *Nano Lett.* **2005**, *5*, 2139−2143.
(17) Wagner, R. S.; Ellis, W. C. *Appl. Phys. Lett.* **1964**, *4*, 89−90.
(18) Eichfeld, S. M.; Ho, T.-T; Eichfeld, C. M.; Cranmer, A.; Mohney, S. E.; Mayer, T. S.; Redwing, J. M., *Nanotechnology* **2007**, *18*, 315201.
(19) Bard, A. J.; Bocarsly, A. B.; Fan, F. R. F.; Walton, E. G.; Wrighton, M. S. *J. Am. Chem. Soc.* **1980**, *102*, 3671−3677.
(20) Bocarsly, A. B.; Bookbinder, D. C.; Dominey, R. N.; Lewis, N. S.; Wrighton, M. S. *J. Am. Chem. Soc.* **1980**, *102*, 3683−3688.
(21) Lewis, N. S. *J. Electro. Chem. Soc.* **1984**, *131*, 2496−2503.

JA073125D